Path Loss Analysis and Modeling for Vehicle-to-Vehicle Communications in Convoys in Safety-related Scenarios

Pan Tang*‡, Rui Wang†‡, Andreas F. Molisch‡, Chen Huang§‡, Jianhua Zhang*
* State Key Lab of Networking and Switching Technology, Beijing University of Posts and Telecommunications, Beijing, China
† Samsung Research America, Mountain View, California
‡ Ming Hsieh Department of Electrical Engineering, University of Southern California, Los Angeles, CA, USA
§ State Key Lab of Rail Traffic Control and Safety, Beijing Jiaotong University, Beijing, China
{tangpan27, jhzhang}@bupt.edu.cn, {molisch, wang78, ch_628}@usc.edu

***Abstract*—Detailed understanding of vehicle-to-vehicle (V2V) channels is a prerequisite for the design of V2V communication systems. An important application of such communications systems is automated control of vehicles driving in convoy formation, which improves transportation efficiency and reduces traffic jams. In this paper, we analyze and model the path loss characteristics for V2V communications in safety-related convoy scenarios based on a series of channel measurements at 5.9 GHz. The measurements focus on two types of safety-related scenarios. In the first scenario, the convoy formation is broken due to changing traffic lights at an intersection. In the second scenario, the convoy link is obstructed temporarily by trucks or pedestrians. We analyze the signal power (pathloss and shadowing) for both of these scenarios. It is found that street signs, trunks, pedestrians or bushes can bring additional signal attenuation, with trucks providing some 15 dB attenuation and pedestrians providing 7 $\sim$ 10 dB attenuation.**

I. Introduction

Vehicle-to-vehicle (V2V) communications systems have attracted much attention because they can improve road safety and reduce the number of accidents. Especially, as self-driving cars have become popular in recent years, V2V communications become more and more important [1]. V2V communication is the wireless transmission of information and data between cars on the road. The wireless channel is the medium over which this communication occurs, and thus plays an important role in the simulation and performance evaluation of V2V communication systems [2]. Furthermore, the most important characteristic of wireless channels is the path loss because it determines communication range as well as network interference and scalability [3].

In recent years, a lot of research on V2V channels has been carried out [4]–[8]. Path loss analysis and modeling in V2V channels in multiple bands, e.g., 2.3, 5.25, 5.6, 6.75 and 73 GHz, were provided in Refs. [6], [8]–[10]. For example, [9] presented the results on path loss for V2V communications in street intersections, a scenario especially important for collision avoidance applications. The results were derived from a channel measurement in the scenario where two cars are approaching an intersection on a collision course at 5.6 GHz. However, most typical V2V applications operate in the 5.9 GHz band. In Refs. [3], [11]–[15], V2V channel measurements were conducted in 5.9 GHz and path loss models based on measurements were provided in different scenarios. [3] presented parameterized path loss models under line-of-sight (LoS) conditions in four different propagation environments: highway, rural, urban, and suburban, and showed that the path loss exponent is small. [11] developed a non-line-of-sight (NLoS) path loss model for V2V communications based on channel measurements in suburban and urban intersections. [15] presented an alternative NLoS path loss model based on channel measurements in two urban intersections. [14] analyzed the path loss for V2V communications with vehicle obstructions and found that small-vehicle obstruction does not significantly affect the mean of the path loss while large vehicle obstruction brings about 10 dB of additional path loss. And [12] showed that bus osbstruction creates an additional 15 $\sim$ 20 dB path loss.

In this paper, we analyze and model the path loss in safety-related scenarios for V2V communications in convoys. A series of V2V channel measurements were conducted in urban and suburban scenarios at 5.9 GHz. In those measurements, two cars were driving in convoy for most of time. Here, we model the path loss characteristics in the safety-related scenarios where the convoy formation is broken due to change of traffic lights in the intersection, and for the safety-related scenarios where the convoy link is obstructed temporarily by trucks and pedestrians, the path loss variation is analyzed. Furthermore, aided by the angular power spectrum given by multipath estimates from Rimax, a high-resolution parameter estimation (HRPE) algorithm [16], the environment-specifc variations of the path loss are analyzed.

The rest of this paper is organized as follows. Section II introduces the measurement setup. The analysis and modeling of the path loss characteristics are shown in Section III. Finally, Section IV concludes this paper.

II. Measurement setup

A. Measurement system

A real-time continuous MIMO channel sounder was used to conduct V2V channel measurements. This sounder is based

(a) At the TX side.

(b) At the RX side.

Fig. 1. Photes of the antenna arrays on top of the SUVs.

TABLE I
THE KEY PARAMETERS OF THE MEASUREMENT SETUP.

Parameter	Value
Carrier frequency	5.9 GHz
Bandwidth	15 MHz
Transmit power	26 dBm
Sampling rate	20 MS/s
MIMO signal duration	640 us
Number of bits in ADC	16

on the NI-Universal Software Radio Peripherals (USRP) Reconfigurable I/O (RIO) software defined radio platform, and the TX USRP and the RX USRP are synchronized with two Global Position System (GPS)-disciplined rubidium clocks, which provide 1 Pulse Per Second (PPS) for absolute time synchronization. Furthermore, two 8-element vertically polarized uniform circular dipole arrays (VP-UCDA) are connected to the USRPs via electronic switches. These two antenna arrays are mounted on top of two Sport Utility Vehicles (SUVs), i.e., (i): a gray Dodge Journey Mid-size cross-over SUV in Fig. 1(b), and (ii): a red Hyundai Sante Fe Mid-size SUV, as shown in Fig. 1(a). A back-to-back system calibration is performed to remove the effects of the measurement system on the measured data. Detailed descriptions of this sounder can be found in [17].

In measurements, this sounder transmitted a Orthogonal Frequency Division Multiplexing (OFDM)-like sounding signal around 5.9 GHz with a bandwidth of 15 MHz. The signal was applied by electronic switches to the different TX antenna elements in sequence; similarly the RX antenna elements were connected to the receive Software Defined Radio (SDR) in a round-robin manner such that all combinations of TX and RX antenna elements were sounded within the MIMO signal duration of 640 μs. The output power was about 26 dBm. The channel transfer function is recorded continuously. The TX and RX vehicles were driving in convoy for most of time. Their GPS locations were recorded in real-time so that the distance between the TX and the RX can be estimated. Two 360° panoramic video cameras were positioned on top of the TX and RX antenna arrays during the measurements, in order to document the scenarios, routes, and special events such as blockage by trucks. The key parameters of the measurement setup are given in Table I.

B. Measurement scenarios

The V2V channel measurements were conducted in and around the University Park Campus of the University of Southern California (USC). In this paper, we focus on two types of safety-related scenarios. In the first, the convoy formation is broken down due to traffic lights in the intersection. Three sub-scenarios are described as follows:

- Sub-scenario 1: This sub-scenario is located to the west of USC and its GPS coordinates are $34^\circ 01' 23.1'' \text{N}, 118^\circ 17' 37.8'' \text{W}$. In the measurements, the RX stopped in front of the intersection and the TX turned right onto the West 36th Street as shown in Fig. 2(a). This is a sub-urban scenario and buildings around the intersection are one or two-story high. A stop sign and a bush beside the RX may obstruct the signal.
- Sub-scenario 2: This sub-scenario is located on the USC campus and its GPS coordinates are $34^\circ 01' 16.5'' \text{N}, 118^\circ 17' 22.5'' \text{W}$. We can see from Fig. 2(b) that in the measurements, RX stopped in front of the intersection and TX turned left onto the Downey Way. Also some other cars passed through the link between the TX and the RX. Compared to sub-scenario 1, buildings around the intersection are higher. Furthermore, there is a stop sign on the left side of the road.
- Sub-scenario 3: This sub-scenario is also located in the USC campus and its GPS coordinates are $34^\circ 01' 16.3'' \text{N}, 118^\circ 17' 22.0'' \text{W}$. Fig. 2(c) shows the photo of this sub-scenario. In the measurements, the RX stopped behind a truck, which stopped in front of the intersection, and the TX turned right onto McClintock Avenue. Generally, the signal was completely obstructed in this sub-scenario.

Another type of safety-related scenarios is that the convoy link is obstructed temporarily by trucks and pedestrians. There are 2 sub-scenarios as follows:

- Sub-scenario 4: This sub-scenario is located to the north of the USC campus and its GPS coordinates are $34^\circ 01' 31.6'' \text{N}, 118^\circ 17' 25.4'' \text{W}$. As shown in Fig. 3(a), the TX was trying to merge into the lane of the convoy, between the TX and RX. After that, the convoy link was obstructed by the truck.
- Sub-scenario 5: This sub-scenario is located on the USC campus and its GPS coordinates are $34^\circ 01' 27.6'' \text{N}, 118^\circ 17' 15.4'' \text{W}$. From Fig. 3(b), we can see that the RX stopped in front of the intersection due to that three persons were walking through the intersection.

III. Analysis and Modeling of the Path Loss

A. Path loss derivation

After measurement data evaluation using Rimax, a HRPE algorithm, we can obtain the parameters of multipath components (MPCs), like amplitude, delay, Doppler shift, angle of departure (AoD) and angle of arrival (AoA). Details about the

(a)

(b)

(c)

Fig. 2. The first type of safety-related scenarios. There are 3 sub-scenarios: (a) stop signs and trees blocks the signal; (b) buildings are around the intersection and there is a stop sign on the left side of the road; (c) signal is obstructed by the building and there is a truck in front of the RX. The red arrow points to the direction that TX turns onto.

(a)

(b)

Fig. 3. The second type of safety-related scenarios. There are 2 sub-scenarios: (a) the convoy link is obstructed by the truck; (b) the convoy link is obstructed by the pedestrian.

HRPE algorithm can be found in [16]. The path loss at time t can be obtained as

$$PL(t)[\text{dB}] = -10\log_{10}\sum_{n=1}^{N_t}|a_n(t)|^2, \tag{1}$$

where N_t is the number of MPCs at time t, $a_n(t)$ is the amplitude of the nth MPC at time t. During measurements, GPS coordinates of the TX and the RX were recorded in real-time. Thus each time sample can be converted to the corresponding distance sample, i.e., $PL(d)$ (d is the distance between the TX and the RX).

B. Analysis and modeling

The floating intercept (FI) path loss model is used here to model the path loss [18].

$$PL(d)[\text{dB}] = \alpha + 10\beta\log_{10}(d) + X_\sigma, \tag{2}$$

where α is the floating intercept, β is the path loss exponent, and X_σ is a zero mean Gaussian random variable that represents the shadow fading. For comparison, path loss in free space at 5.9 GHz can be written as [19]

$$PL(d)[\text{dB}] = 47.86 + 20\log_{10}(d). \tag{3}$$

Firstly, we analyze and model the path loss in the first scenario type. Fig. 4 shows the path loss results in the first sub-scenario, with the free-space pathloss plotted for comparison. We can see that there is an offset (about 10 dB in the beginning) between the two curves. This offset mainly results from the obstruction by the stop sign and the bush, see Fig. 2(a). The path loss exponent is about 2.47, which indicates that signal experiences larger attenuation in this sub-scenario than in free space after spreading the same distance.

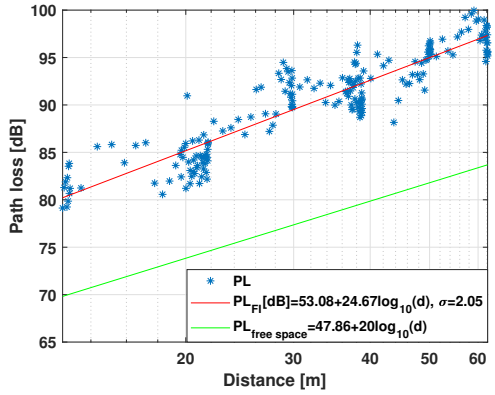

Fig. 4. The path loss results in the first sub-scenario.

Fig. 5 displays the path loss results in the second sub-scenario. The fitted floating intercept is about 45 dB, which is close to that in free space. The fitted path loss exponent is about 2.56. Basically, the measured path loss is close to that in free space. On the other hand, we can see that the path loss has relatively large variance along the distance. To better explain this phenomenon, the angular spectrum of MPCs obtained using Rimax is given in Fig. 7[1]; Fig. 6 shows the angular coordinates of the TX and the RX in the second sub-scenario. The angle range is from $-180°$ to $180°$. For both the TX and the RX, $0°$ is the forward driving direction. It is easy to find that the AoA and AoD of the LoS path are about $60°$ and $150°$, respectively. Furthermore, the LoS path experiences additional attenuation in the red circles shown in Fig. 7. Besides, this is the reason why the path loss has a relatively variance shown in Fig. 5. According to the recorded video, the attenuation in circle 1 is caused by the stop sign; the attenuation in circle 2 is caused by the passing car, which can be found in Fig. 2(b). Compared to the results in the first sub-scenario, we can see that passing cars are more likely to obstruct the LoS path when the car in convoy turns left than when the car in convoy turns right. It is also noteworthy that objects such as stop signs, which are usually not found in geographical databases, have such a significant impact on the receive power; this has important implications, e.g., for ray tracing analysis of such scenarios.

Fig. 8 shows the path loss results in the third sub-scenario. The fitted path loss exponent, about 3.45, is much larger than

[1]The raw data used for plotting Fig. 7 is the same as that used for plotting Fig. 5.

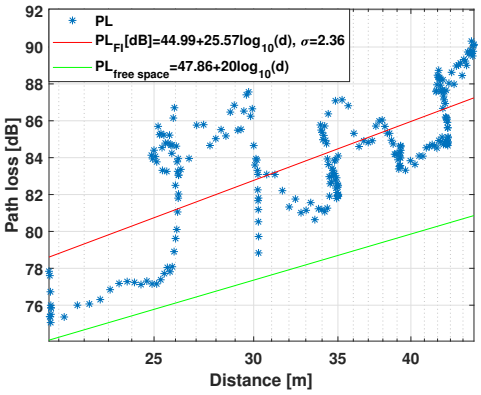

Fig. 5. The path loss results in the second sub-scenario.

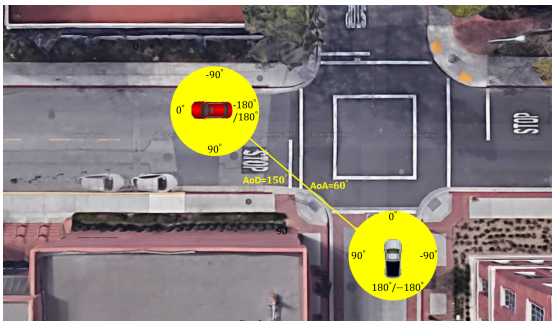

Fig. 6. The angular coordinates of the TX and the RX in the second sub-scenario.

that in other sub-scenarios, and we can see a big offset (about 24 dB at the beginning) between the measured path loss and the free space path loss, as well as larger than the offset in the first and the second sub-scenarios. This is basically because the truck and the building beside the road shown in Fig. 2(c) obstruct the LoS path.

Next, we analyze the path loss in the second type of safety-related scenarios. Since the variance of TX-RX distance in this case is very small, it is more meaningful to present the path loss as a function of time. Fig. 9 demonstrates the path loss results in the fourth sub-scenario. At time 882 s, the TX was trying to merge as shown in Fig. 3(a). After waiting for a few seconds due to the traffic, the TX merged successfully. In this process, we can see that the path loss increases about 16.5 dB. This attenuation is mostly caused by the truck between the TX and the RX. In Ref. [12], an additional 15-20 dB attenuation caused by a large vehicle was also investigated.

Fig. 10 shows the path loss results in the fifth sub-scenario. We can see that there are two peaks in the red circles. The left peak is caused by two pedestrians walking side-by-side across the road, while the right peak is caused by the third pedestrian in the back, see Fig. 3(b). Furthermore, the average path loss from 1104 s to 1107 s is about 79.5 dB, which can be a reference to calculate the attenuation caused by the pedestrian. Empirically, the attenuation caused by the first two pedestrians is about 7.68 dB while the attenuation caused by

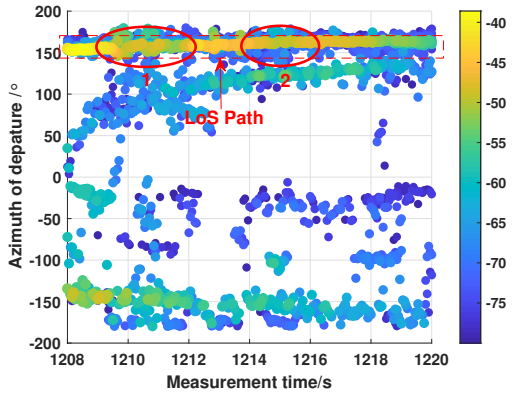

(a)

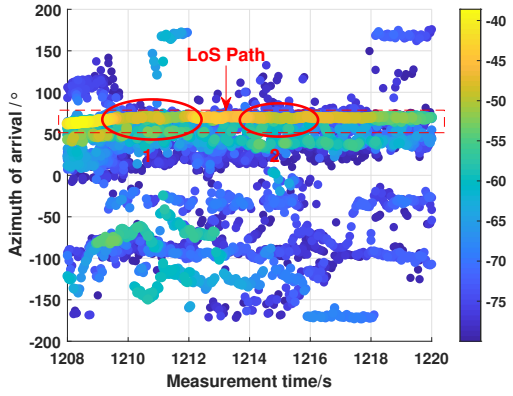

(b)

Fig. 7. The angular spectrum of MPCs in the second sub-scenario at: (a) the TX; (b) the RX.

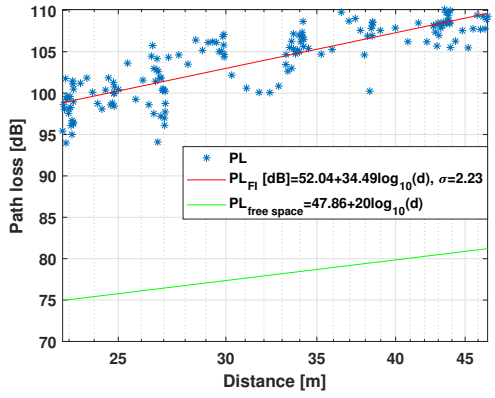

Fig. 8. The path loss results in the third sub-scenario.

the third pedestrian is about 10.16 dB. To further demonstrate the above analysis, Fig. 11 shows the angular spectrum of MPCs within the same period. Combining Fig. 3(b) and Fig. 6, it is easy to see that the AoA and AoD of the LoS path are about 0° and 180° (or -180°), respectively. And the LoS path is obstructed temporarily by the pedestrian at around 1103 s and 1108 s. This agrees with the observation in Fig. 10.

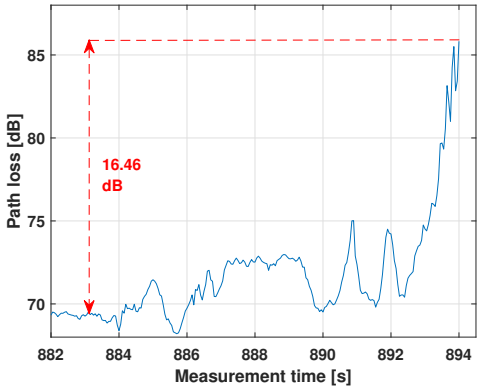

Fig. 9. The path loss results in the fourth sub-scenario.

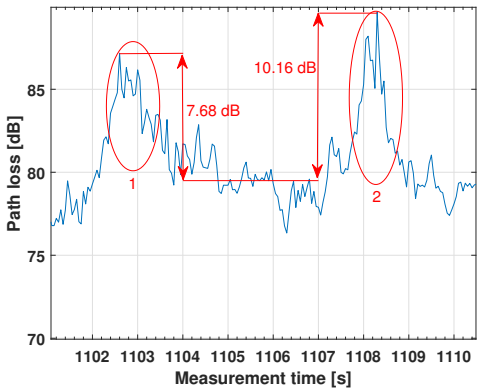

Fig. 10. The path loss results in the fifth sub-scenario.

IV. Conclusion

Based on the V2V channel measurements conducted in and around the USC campus, we analyzed and modeled the path loss for V2V communication in convoys in safety-related scenarios. Not surprisingly, we found that environments have a strong effect on the path loss. For example, street signs and bushes can bring additional path loss, and if the distance between the street sign and the car is small, the attenuation is more severe. Also the direction that the leading vehicle turns to affects the signal attenuation characteristics: cars turning left are more likely to experience more dynamic attenuation because the passing cars from the opposite direction can obstruct the convoy link. Finally, our measurements have also shown that the truck obstruction can cause attenuation about 15 dB to the convoy communication link, and pedestrians can cause about 7 $\sim$ 10 dB attenuation. These results are helpful for the system simulation and performance evaluation of V2V communication systems.

Acknowledgment

The work of Pan Tang and Jianhua Zhang is supported in part by National Science and Technology Major Project (No.2018ZX03001031), Natural Science Foundation of Beijing (No.L172030), Beijing Municipal Science & Technology

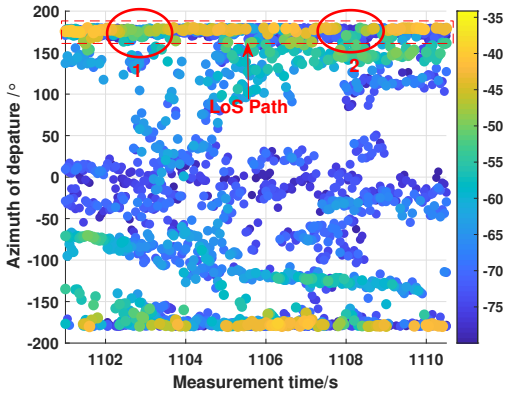

(a)

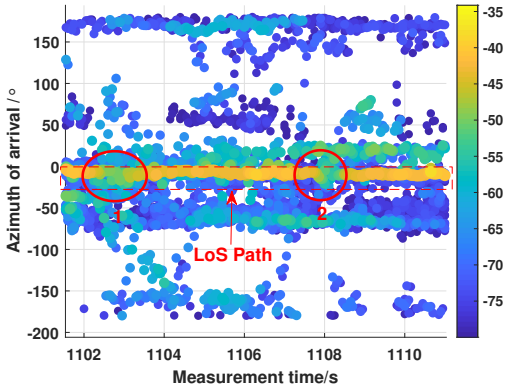

(b)

Fig. 11. The angular spectrum of MPCs in the fifth-scenario at: (a) the TX; (b) the RX.

Commission Project (No.Z181100003218007), Key Project of State Key Lab of Networking and Switching Technology (NST20170205), and National Key TechnologyResearch and Development Program of the Ministry of Science and Technology of China (NO. 2012BAF14B01). The work of Rui Wang and Andreas F. Molisch was supported by the California Transportation Authority under a METRANS project, and the National Science Foundation.

REFERENCES

[1] P. Gora and I. Rüb, "Traffic models for self-driving connected cars," *Transportation Research Procedia*, vol. 14, pp. 2207–2216, 2016.

[2] A. F. Molisch, F. Tufvesson, J. Karedal, and C. F. Mecklenbrauker, "A survey on vehicle-to-vehicle propagation channels," *IEEE Wireless Communications*, vol. 16, no. 6, pp. 12–22, December 2009.

[3] J. Karedal, N. Czink, A. Paier, F. Tufvesson, and A. F. Molisch, "Path loss modeling for vehicle-to-vehicle communications," *IEEE Transactions on Vehicular Technology*, vol. 60, no. 1, pp. 323–328, Jan 2011.

[4] M. Yang, B. Ai, R. He, L. Chen, X. Li, J. Li, Q. Wang, B. Zhang, and C. Huang, "A cluster-based 3d channel model for vehicle-to-vehicle communications," in *2018 IEEE/CIC International Conference on Communications in China (ICCC)*. IEEE, 2018, pp. 741–746.

[5] Y. Chakkour, H. Fernández, V. M. R. Peñarrocha, L. Rubio, and J. Reig, "Coherence time and doppler spread analysis of the v2v channel in highway and urban environments," in *2018 IEEE International Symposium on Antennas and Propagation & USNC/URSI National Radio Science Meeting*. IEEE, 2018, pp. 373–374.

[6] M. Boban, D. Dupleich, N. Iqbal, J. Luo, C. Schneider, R. Müller, Z. Yu, D. Steer, T. Jämsä, J. Li *et al.*, "Multi-band vehicle-to-vehicle channel characterization in the presence of vehicle blockage," *IEEE Access*, vol. 7, pp. 9724–9735, 2019.

[7] Q. Wang, B. Ai, R. He, M. Yang, B. Zhang, J. Li, L. Chen, and X. Li, "Time-variant cluster-based channel modeling for v2v communications," in *2018 IEEE International Conference on Communications (ICC)*. IEEE, 2018, pp. 1–6.

[8] H. Wang, X. Yin, X. Cai, H. Wang, Z. Yu, and J. Lee, "Fading characterization of 73 ghz millimeter-wave v2v channel based on real measurements," in *Communication Technologies for Vehicles: 13th International Workshop, Nets4Cars/Nets4Trains/Nets4Aircraft 2018, Madrid, Spain, May 17-18, 2018, Proceedings 13*. Springer, 2018, pp. 159–168.

[9] J. Karedal, F. Tufvesson, T. Abbas, O. Klemp, A. Paier, L. Bernadó, and A. F. Molisch, "Radio channel measurements at street intersections for vehicle-to-vehicle safety applications," in *2010 IEEE 71st Vehicular Technology Conference*. IEEE, 2010, pp. 1–5.

[10] A. Roivainen, P. Jayasinghe, J. Meinila, V. Hovinen, and M. Latva-aho, "Vehicle-to-vehicle radio channel characterization in urban environment at 2.3 ghz and 5.25 ghz," in *2014 IEEE 25th Annual International Symposium on Personal, Indoor, and Mobile Radio Communication (PIMRC)*. IEEE, 2014, pp. 63–67.

[11] T. Abbas, A. Thiel, T. Zemen, C. F. Mecklenbräuker, and F. Tufvesson, "Validation of a non-line-of-sight path-loss model for v2v communications at street intersections," in *2013 13th International Conference on ITS Telecommunications (ITST)*. IEEE, 2013, pp. 198–203.

[12] R. He, A. F. Molisch, F. Tufvesson, Z. Zhong, B. Ai, and T. Zhang, "Vehicle-to-vehicle propagation models with large vehicle obstructions," *IEEE Transactions on Intelligent Transportation Systems*, vol. 15, no. 5, pp. 2237–2248, 2014.

[13] B. Kihei, J. A. Copeland, and Y. Chang, "Improved 5.9 ghz v2v short range path loss model," in *2015 IEEE 12th International Conference on Mobile Ad Hoc and Sensor Systems*. IEEE, 2015, pp. 244–252.

[14] M. Yang, B. Ai, R. He, L. Chen, X. Li, Z. Huang, J. Li, and C. Huang, "Path loss analysis and modeling for vehicle-to-vehicle communications with vehicle obstructions," in *2018 10th International Conference on Wireless Communications and Signal Processing (WCSP)*. IEEE, 2018, pp. 1–6.

[15] M. Nilsson, C. Gustafson, T. Abbas, and F. Tufvesson, "A path loss and shadowing model for multilink vehicle-to-vehicle channels in urban intersections," *Sensors*, vol. 18, no. 12, p. 4433, 2018.

[16] R. Wang, O. Renaudin, C. U. Bas, S. Sangodoyin, and A. F. Molisch, "High-resolution parameter estimation for time-varying double directional v2v channel," *IEEE Transactions on Wireless Communications*, vol. 16, no. 11, pp. 7264–7275, 2017.

[17] R. Wang, C. U. Bas, O. Renaudin, S. Sangodoyin, U. T. Virk, and A. F. Molisch, "A real-time mimo channel sounder for vehicle-to-vehicle propagation channel at 5.9 ghz," in *2017 IEEE International Conference on Communications (ICC)*. IEEE, 2017, pp. 1–6.

[18] G. R. MacCartney, J. Zhang, S. Nie, and T. S. Rappaport, "Path loss models for 5g millimeter wave propagation channels in urban microcells." in *Globecom*, 2013, pp. 3948–3953.

[19] A. F. Molisch, *Wireless communications*. John Wiley & Sons, 2012, vol. 34.